Clays and Clay Minerals, Vol. 51, No. 1, 41–51, 2003.

PREPARATION AND CHARACTERIZATION OF Ti-PILLARED CLAYS USING Ti ALKOXIDES. INFLUENCE OF THE SYNTHESIS PARAMETERS

JOSÉ LUIS VALVERDE*, PAULA SÁNCHEZ, FERNANDO DORADO, ISAAC ASENCIO AND AMAYA ROMERO

Facultad de Ciencias Químicas, Departamento de Ingeniería Química, Universidad de Castilla-La Mancha, 13004 Ciudad Real, Spain

Abstract—Titanium was introduced into the clay structure by cation exchange with polymeric Ti cations which were formed by partial hydrolysis of Ti alkoxide in HCl. X-ray diffraction, N_2 adsorption-desorption, chemical analysis, thermogravimetric analysis, differential thermal analysis, temperature-programmed desorption of ammonia and temperature-programmed reduction were used to characterize the resulting Ti-pillared clays (Ti-PILCs). Titanium methoxide allows the synthesis of a solid with a large basal spacing (26 Å), a large surface area (360 m^2/g), a significant amount of micropore surface area (90%), and notable acidity. Moreover, Ti-PILCs obtained from methoxide were found to be thermally stable up to 500ºC. A correlation between the increase in acidity and the increases in both microporosity and Ti content was observed. The surface area, the micropore volume, the acidity and the d_{001} peak intensity all increased upon increasing the amount of Ti added to the preparation (up to ~15 mmoles of Ti/g clay). The use of an aqueous suspension of 0.13 wt.% of clay yielded the best structural and textural properties in terms of subsequent use of the clay as a catalyst.

Key Words—Acidity, Basal Spacing, Pillared Clay, Synthesis, Titanium Alkoxides.

INTRODUCTION

The escalation of oil prices in 1973 confronted the oil industry with the problem of how to maximize the processing of crude oil, especially the heavy fractions, to give gasoline components. A strong emphasis was thus placed on the development of catalysts with relatively large pore sizes, which are able to deal with larger molecules than the existing molecular sieves, and good thermal and hydrothermal stability. The search for such systems resulted in renewed interest in the concept of pillared clays. The use of inorganic hydrated polyoxocations as pillaring agents provided thermally stable pillared clays with large specific surface areas (Kloprogge, 1998).

On the other hand, in recent years, the suitability of pillared clays for use in catalyst support has been explored, especially because of the textural and acidic properties of these solids. Titanium-pillared intercalated clays (Ti-PILCs) have been used extensively as catalysts for the selective catalytic reduction of NO*x* (Del Castillo *et al.*, 1996; Li *et al.*, 1997; Long and Yang, 2000).

Pillared clays are two-dimensional zeolite-like materials prepared by exchanging charge-compensating cations between the clay layers with large inorganic metal hydroxycations, which are oligomeric and are formed by hydrolysis of metal oxides or salts (Baes and Mesner, 1976). After calcination, the metal hydroxycations are decomposed into oxide pillars that keep the clay layers apart and create interlayer and interpillar spaces, thereby exposing the internal surfaces of the clay layers. The polyoxymetal cations apparently aggregate to form cationic oligomers in solution. The size of these oligomers appears to control the size of the pore openings in the pillared clay. In principle, any metal oxide or salt that forms polynuclear species upon hydrolysis can be inserted as a pillar (Baes and Mesner, 1976; Burch, 1988; Clearfield, 1994; Sprung *et al.*, 1990; Shabtai *et al.*, 1984).

Intercalated clays are usually natural smectite clays. Smectite clays are readily pillared because of their low charge density and their swelling ability (Cañizares, 1999). Properties such as acidity, surface area, pore-size distribution and hydrothermal stability depend on the method of synthesis as well as on the nature of the host clay.

The main studies aimed at the application of pillared clays have, not surprisingly, concerned heterogeneous catalysts. Additional applications have been found in fields as diverse as environmental uses, thermal insulators, pigments, electrodes and membranes (Purnell, 1990).

In spite of the interesting catalytic properties of Ti-based catalysts, Ti-PILCs have received considerably less attention than other pillared clays. Titanium has been known for quite some time to form polymeric species in solution (Nabivanets and Kudritskaya, 1967; Einaga, 1979). In general, two different methods to create Ti complexes suitable for pillaring processes have been reported in the literature (Bovey *et al.*, 1996; Kooli *et al.*, 1997; Vicente *et al.*, 2001). The first approach to the preparation of Ti complexes in solution is the addition of $TiCl_4$ to HCl, followed by dilution with distilled water and ageing for several hours prior to use

* E-mail address of corresponding author:
jlvalver@inqu-cr.uclm .es
DOI: 10.1346/CCMN.2003.510105

as a pillaring agent (Yang *et al.*, 1992; Sterte, 1986; Bernier *et al.*, 1991). The second approach is based on the hydrolysis of Ti alkoxides in a HCl medium (Malla *et al.*, 1989). Both methods have proven to be suitable for the preparation of Ti-PILCs although the first requires careful handling of the $TiCl_4$. The resulting Ti-PILCs are solids that present a very ordered arrangement in their structure and have a basal spacing of ~25 Å. These materials have a structure consisting of sheets separated by small TiO_2 particles – though large enough to allow the adsorption of different compounds. The most important difference between Ti-PILCs and other metal-PILCs is the considerably larger interlayer spacing of the Ti materials. The interlayer spacing of Ti-PILCs is ~16 Å compared with ~10 Å for Al-PILCs or Zr-PILCs (Lahav *et al.*, 1978; Yamanaka and Brindley, 1979). The larger interlayer distance in the Ti systems is accompanied by a thermal and hydrothermal stability comparable with that of Al-PILCs and Zr-PILCs (Sterte, 1986).

In the work described here we studied the preparation of Ti-pillared clays and present detailed results aimed at elucidating (1) the influence of the Ti alkoxide used as a starting material, (2) the influence of the amount of Ti added in the pillaring procedure, and (3) the influence of the suspension clay concentration. Extensive results on the properties and physicochemical characteristics of the Ti-PILCs are also presented.

EXPERIMENTAL

Preparation of Ti-PILCs

The clay used as the starting material in the synthesis of Ti-PILCs was a purified bentonite (particle size <2 μm) was supplied by Fisher Scientific with the chemical analysis (wt.%): SiO_2, 52.22; Al_2O_3, 16.81; Fe_2O_3, 3.84; Na_2O, 1.26; MgO, 0.88; CaO, 0.74; K_2O, 0.80. The CEC (cation exchange capacity) was determined by dispersing the clay and then saturating with K^+ ions using 1 N KCl. The amount of exchanged K^+ was determined by atomic absorption and found to be 94 meq/100 g clay.

The first step in the synthesis of Ti-PILCs is the preparation of the pillaring solution in which the oligomeric Ti species are formed. In this method the appropriate Ti alkoxide was added to a 5 N HCl solution. This solution was aged under stirring at room temperature for 3 h. The subsequent step involved exchange of the cations situated between the clay layers with the previously formed oligomers. In order to achieve this exchange, an original clay suspension was prepared with deionized water. The pillaring Ti solution was slowly added to the clay suspension with vigorous stirring. The mixture was allowed to react with stirring at room temperature for 12 h. After this time period had elapsed, the solid was separated from the solution by centrifugation and then washed with deionized water until chloride free (i.e. the conductivity of the washing water was <10 μS/cm). The aim of the washing stage was to remove excess Cl^- ions which prevent diffusion of the polyoxocations within the interlayer space (Pesquera *et al.*, 1991). The solid was air dried and the resulting product was calcined for 2 h at different temperatures. The conditions used for the preparation of the materials and the corresponding notation for each sample are given in Table 1. For instance, Ti-Met-10-0.10 corresponds to a sample synthesized using Ti methoxide, 10 mmoles of Ti per gram of clay, and a suspension clay concentration of 0.10 wt.%.

Characterization techniques

The X-ray diffraction (XRD) patterns were obtained using a Philips PW 1710 diffractometer with Ni-filtered CuKα radiation. In order to maximize the 001 reflection intensities, oriented clay-aggregate specimens were prepared by drying clay suspensions on glass slides. The XRD pattern of the parent clay exhibits a peak at ~9º, commonly assigned to the basal 001 reflection (d_{001}). In pillared clays, the d_{001} peak was found to shift towards the lower 2θ region, which is a clear indication of the enlargement of the basal spacing of the clay. The thermal stability of samples was investigated by exposing the materials to temperatures in the range 200–500ºC for 2 h in air.

Surface area and pore-size distribution were determined by using N as the sorbate at 77 K in a static volumetric apparatus (Micromeritics ASAP 2010 sorptometer). Pillared clays were outgassed prior to use at

Table 1. Experimental conditions used in the preparation of Ti-PILCs.

Sample designation	Ti alkoxide	mmol Ti/g clay	Suspension clay concentration (wt.%)
Ti-Met-10-0.10	Methoxide	10	0.10
Ti-Eth-10-0.10	Ethoxide	10	0.10
Ti-Pro-10-0.10	Propoxide	10	0.10
Ti-But-10-0.10	Butoxide	10	0.10
Ti-Met-5-0.10	Methoxide	5	0.10
Ti-Met-15-0.10	Methoxide	15	0.10
Ti-Met-25-0.10	Methoxide	25	0.10
Ti-Met-15-0.13	Methoxide	15	0.13
Ti-Met-15-0.20	Methoxide	15	0.20

https://doi.org/10.1346/CCMN.2003.510105 Published online by Cambridge University Press

180ºC for 16 h under a vacuum of 6.6×10^{-9} bar. Specific total surface areas were calculated using the BET equation, whereas specific total pore-volumes were evaluated from N_2 uptake at a relative pressure (P/P_o) of N_2 equal to 0.99. The Horvath–Kawazoe method was used to determine the microporous surface area and micropore volume (Horvath and Kawazoe, 1983). The Barret, Johner and Halenda (BJH) method was used to determine the distributions of the mesopores (Barret *et al.*, 1951).

Thermogravimetric analyses (TGA) were performed on 10 mg samples using a Perkin-Elmer TGA 7 thermogravimetric analyzer under a helium flow of 50 mL min^{-1} and with a heating rate of 15ºC min^{-1} up to 900ºC.

The total acid site density of each of the catalysts was measured by temperature-programmed desorption of ammonia (TPDA) using a Micromeritics TPD/TPR 2900 analyzer with a thermal conductivity detector (TCD). The samples were housed in a quartz reactor and pretreated in a flow of helium while heating at 15ºC/min up to the calcination temperature of the sample. After a period of 30 min at this temperature, the samples were cooled to 180ºC and saturated for 15 min in a stream of ammonia. The catalyst was then allowed to equilibrate in a helium flow at 180ºC for 1 h. The ammonia was then desorbed using a linear heating rate of 15 ºC/min up to 500ºC. Temperature and detector signals were recorded simultaneously. Total acidity is defined as the total acid site density, obtained by integration of the area under the curve.

Temperature programmed reduction (TPR) measurements were carried out with the same apparatus described above. After loading, the sample was outgassed by heating at 15ºC/min in an argon flow up to the calcination temperature of the sample and kept constant at this temperature for 30 min. Next, it was cooled to room temperature and stabilized under an argon/hydrogen flow ($\geqslant$99.9990% purity, 83/17 volumetric ratio). The temperature and detector signals were then continuously recorded while heating at 20ºC/min up to 800ºC. The liquids formed during the reduction process were retained by a cooling trap placed between the sample and the detector. The TPR profiles are reproducible, standard deviations for the temperature of the peak maxima being ±2%.

Changing the experimental TPD/TPR conditions may compensate for external diffusion. Decreasing the ramp rate and increasing the inert gas flow rate both help to close the gap between true and detected desorption/reduction temperatures. The TPD/TPR curves obtained by modifying these experimental conditions were similar to those presented in this work, so the process was not external-diffusion controlled.

The Ti loading (wt.%) of the prepared materials was determined by atomic absorption spectroscopy using a SPECTRAA 220 FS analyzer.

RESULTS AND DISCUSSION

Effect of the titanium alkoxide

Figure 1a shows the XRD patterns of the original clay and the Ti-PILCs which were prepared using the following Ti alkoxides: methoxide, ethoxide, propoxide, and butoxide. It can be seen that the d_{001} peak appears at smaller 2θ angles than that of the original clay. This clearly indicates an enlargement of the basal spacing of the clay as a consequence of the pillaring process. Moreover, this peak is quite intense in the four solids prepared, suggesting that the pillaring process yielded solids with a uniform and stable structure. It should also be noted that a wider peak, which is less intense than the first one, appears at 7º2θ. This peak has also been observed for Ti-PILCs reported by other authors and suggests the presence of a proportion of the clay exchanged with some type of monomeric Ti species (smaller in size) (Kloprogge, 1998), a situation that leads to a smaller opening of the clay layers.

Figure 2a shows the XRD patterns of the sample Ti-Met-10-0.10 calcined at different temperatures. It can be seen that the peak at 4º2θ becomes more defined and more intense as the calcination temperature increases. In contrast, the peak at 7º2θ becomes broader and less intense. This result could be due to the existence of different hydration states, to the crystallization of the Ti polyoxocations, to the loss of the adsorbed hydration water or even to the different structures of Ti oxide that could generate a more homogeneous pillar distribution (Bahranowski and Serwicka, 1993).

The basal spacing values of the synthesized samples, calcined at different temperatures, are given in Table 2. The interlayer spacing for Na-montmorillonite is ~3.5 Å, and the interlayer spaces are occupied by hydrated Na^+ cations. The structure collapses after dehydration (d_{001} decreased to 9.7 Å) and the interlayer region becomes inaccessible to the N_2 molecules. Large, hydrated Ti polyoxycations introduced into the interlayer spaces of the clay push the sheets apart by ~14.4 Å (*i.e.* the d_{001} value of 24 Å minus 9.6 Å). The texture of the resulting clay is open and is accessible to adsorbate molecules. The specific surface area of the mineral increases tenfold in relation to that of the starting clay and is a measure of both the internal (prevailing) and external surface (Sun Kou *et al.*, 2000). Calcination of the Ti-pillared clays leads to dehydration and dehydroxylation of Ti polycations and gives rise to the formation of polymeric TiO_2 species which permanently link adjacent sheets. The distance between the sheets of these pillared clays hardly decreases and the structure of the minerals still remains open up to 500ºC. These results indicate that the solids prepared not only have a great thermal stability, but their structure becomes more uniform, stable and regular. Similar basal spacing values were observed for the samples synthesized using different Ti alkoxides, apart from the increase seen when Ti methoxide was used. It is

https://doi.org/10.1346/CCMN.2003.510105 Published online by Cambridge University Press

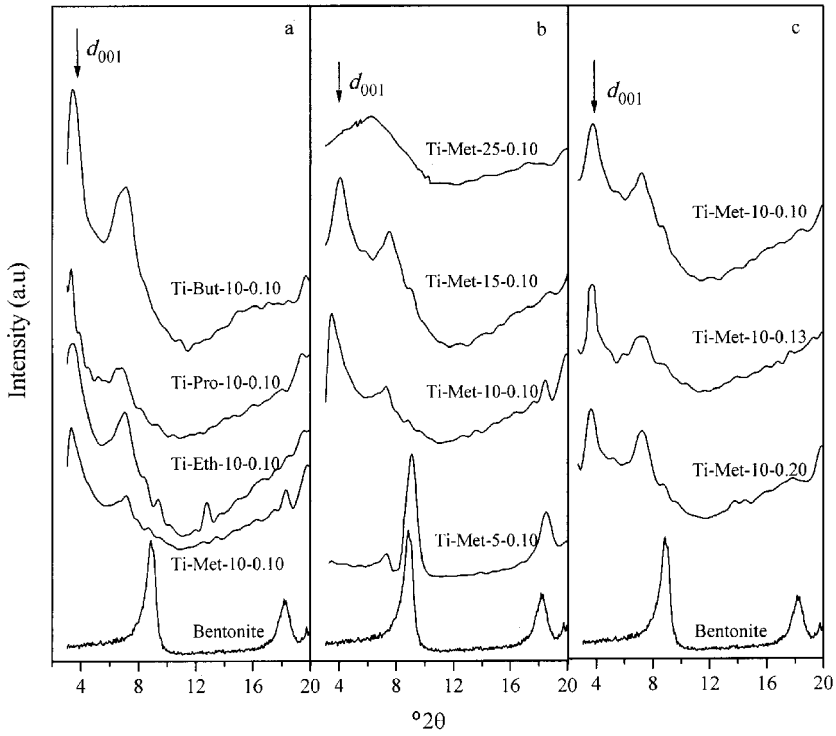

Figure 1. XRD patterns of Ti-PILCs prepared under different conditions calcined at 500ºC. (a) Effect of Ti alkoxide, (b) effect of the amount of Ti, and (c) effect of the clay suspension.

known that the nature of the alkoxide group is a very important parameter in the hydrolysis and condensation to obtain metal oxides (Del Castillo *et al.*, 1997). The ease with which the alkoxy group can be exchanged should decrease with the length of the chain and this would affect the structure of the resulting Ti oxide. This fact could explain the larger basal spacing obtained when Ti methoxide was used.

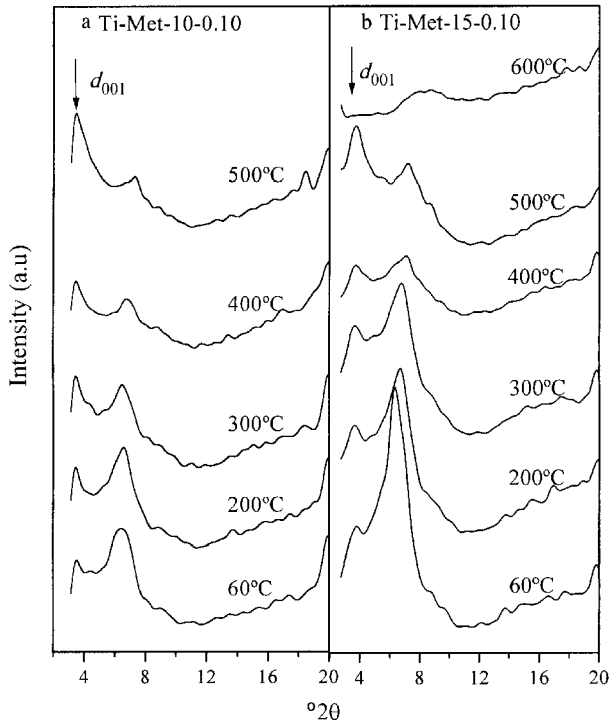

Figure 2. XRD patterns of (a) Ti-Met-10-0.10, and (b) Ti-Met-15-0.10, calcined at different temperatures.

https://doi.org/10.1346/CCMN.2003.510105 Published online by Cambridge University Press

Table 2. Basal spacing (Å) of Ti-PILCs calcined at different temperatures.

Sample	60ºC	200ºC	300ºC	400ºC	500ºC
Original clay	13.4	9.9	9.8	9.7	9.7
Ti-Met-10-0.10	24.5	25.2	25.4	25.4	25.4
Ti-Eth-10-0.10	23.4	24.2	23.9	23.2	23.0
Ti-Pro-10-0.10	25.2	25.2	25.2	23.9	23.9
Ti-But-10-0.10	23.9	24.5	24.5	23.9	23.9
Ti-Met-5-0.10	12.8	12.6	11.1	10.1	9.7
Ti-Met-15-0.10	23.4	24.7	24.7	24.7	24.7
Ti-Met-25-0.10	21.8	21.8	21.8	21.8	21.8
Ti-Met-15-0.20	25.8	25.1	24.7	24.7	24.7
Ti-Met-15-0.13	25.4	25.4	24.7	24.7	24.7

The textural properties, acidity and Ti content of samples are shown in Table 3. It can be seen that the specific surface area of Ti-PILCs is about nine times larger than that of the original clay, as a consequence of the pillaring process. The sample prepared using Ti propoxide gave the largest amount of micropore area over the total surface area (at 200ºC), as well as the largest Ti content and acidity values (Table 3). According to Sychev (1992), the increased acidity could be due to the occurrence of dealumination during the synthesis of the Ti-pillared clays. In the opinion of other authors, the differences in total acidity, which is greater in the prepared Ti-PILCs, can be attributed both to the weak acidic character of the Ti species acting as pillars and to the significant increase in micropore area after the pillaring process (Del Castillo, 1993). As can be seen from the results in Table 3, the acidity of samples increased both with increasing micropore and Ti contents. The TPD of ammonia and pyridine adsorption/desorption experiments revealed that the acid sites are mainly strong Lewis acid sites. These sites must be located at the interphase between the pillar and the siloxane surface (Bernier *et al.*, 1991; Bagshaw and Cooney, 1993) because TiO_2 itself does not have significant acidity and the observed acidity differs strongly from that of the starting clay. Lewis acidity is generally directly related to the kind and amount of interlayer pillars. In contrast, conclusions reported on the Brønsted acidity are open to discussion and this characteristic seems to depend on the parent clay and on parameters such as pretreatment temperature or outgassing temperature (Chevalier *et al.*, 1994).

Figure 3 shows the variation of the surface area of Ti-PILCs with calcination temperature. The sample Ti-Met-10-0.10 has the largest surface area at 500ºC of the four materials examined. It can be seen for this sample that when the calcination temperature increases the surface area also increases until a temperature of 500ºC is reached after which the surface area begins to decrease. Sample Ti-Eth-10-0.1 showed a similar trend although in this case the maximum surface area occurred at temperatures of ~400ºC. Samples obtained from Ti propoxide and butoxide gave rise to almost constant surface area values up to 400ºC and these values decreased at higher temperatures. Taking into account the fact that different Ti oligomers can be created through the hydrolysis of different alkoxides, the surface area increase that takes place during calcination of the intercalated samples up to a specific temperature, might be explained in part by the thermal decomposition of the alkoxide ligands, which further facilitates access to the porous network of the pillared clays.

According to Zhu *et al.* (1995), the reduction in the surface areas and micropore volumes in PILCs is due to changes in the Hoffman Klemen effect, *i.e.* heating causes irreversible migration of small cations to the vacant octahedral sites in the clay layers and the partial collapse of the structure. This argument does not apply

Table 3. Textural properties, acidity and Ti content of Ti-PILCs.

Sample	Surface area (m^2/g)	Micropore surface area (m^2/g)[1]	Micropore volume (cm^3/g)	Pore volume (cm^3/g)	Acidity (mmol NH_3/g clay)	Ti (wt.%)
Original clay	36.2	15.1	0.0066	0.069	0.132	0.0
Ti-Met-10-0.10	304.6	269.0 (89)	0.1688	0.234	0.537	27.1
Ti-Eth-10-0.10	310.8	280.6 (90)	0.1680	0.221	0.538	28.2
Ti-Pro-10-0.10	345.0	317.5 (92)	0.1994	0.248	0.555	32.3
Ti-But-10-0.10	320.9	288.6 (90)	0.1805	0.239	0.510	25.1
Ti-Met-5-0.10	78.2	43.6 (55)	0.0134	0.097	0.325	7.3
Ti-Met-15-0.10	353.8	321.5 (90)	0.2066	0.261	0.576	30.7
Ti-Met-25-0.10	315.1	262.4 (83)	0.1608	0.242	0.425	31.3
Ti-Met-15-0.13	357.9	327.7 (91)	0.2227	0.274	0.637	33.2
Ti-Met-15-0.20	341.5	311.0 (91)	0.2079	0.259	0.594	32.2

[1] Values in parentheses represent the percentage of micropores relative to the total area.

https://doi.org/10.1346/CCMN.2003.510105 Published online by Cambridge University Press

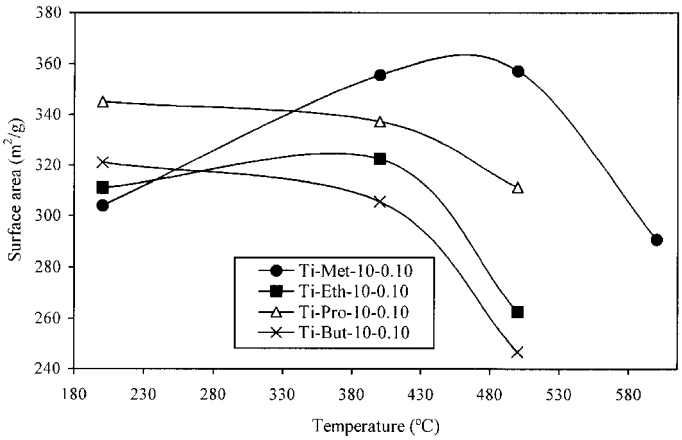

Figure 3. Dependence of surface area upon calcination temperature in Ti-PILCs prepared with different Ti alkoxides.

in the case of the investigated samples since it is very probable that there are no small cations (Li^+ or Mg^{2+}) that could migrate to the octahedral sheet. The main reason for the reduction of the surface area (principally microporous area) at high temperatures is the dehydroxylation and sintering occurring within the structure of pillared clays. These changes seem to be influenced by the nature of the pillared species, which in turn depends on the nature of alkoxide used.

On the basis of the textural characterization and thermal resistance results discussed above, Ti-Met-10-0.1 was selected for the further studies.

Effect of the quantity of Ti per gram of clay

Figure 1b shows XRD patterns of samples (calcined at 500ºC) prepared using 5, 10, 15 and 25 mmoles of Ti/g clay and methoxide as the Ti source. Samples prepared with 10 and 15 mmoles of Ti/g clay had an interlayer spacing ~16 Å larger than the original clay (Table 2), which demonstrates that the pillaring process had taken place. The results show that the differences between the Ti-Met-10-0.1 and Ti-Met-15-0.1 samples are not particularly large (the basal spacing values and the d_{001} peak intensity are similar). Nevertheless, the Ti-Met-5-0.10 sample shows only one main peak at 9º2θ, which is characteristic of the raw clay and indicates that the pillaring process had not taken place – the basal spacing was also quite similar to that of the original clay (9.7 Å) (Table 2). The sample obtained using 25 mmoles of Ti/g clay showed a broad peak (at $2\theta \approx 4-9$º) indicative of a very heterogeneous pillaring process.

The surface area analysis (Table 3) indicates that the pillaring process produces a significant increase in the surface area, from 36.2 m^2/g (typical of the original clay) up to ~300–350 m^2/g, for the Ti-PILCs. This increase is due principally to the formation of micropores (Pesquera *et al.*, 1991). The surface area, pore volume and micropore volume all increase as the Ti content in the pillaring solution is increased (Table 3), reaching a maximum and then decreasing when 25 mmoles Ti/g clay were used. The total acidity increases by approximately a factor of four as a consequence of the pillaring process. It can be seen from the results in Table 3 that a higher Ti content in the pillaring solution leads to a slight increase in the Ti content in the pillared samples (apart from the sample with the smallest amount of Ti). The acidity of the pillared clays increases due to the increase in both Ti content and micropore area. The sample obtained using 25 mmoles Ti/g clay shows a low acidity in spite of the fact that it has the highest Ti content. This situation is due to the fact that its micropore area is less than those of the materials obtained using 10 and 15 mmoles Ti/g clay.

Representative N_2-adsorption/desorption isotherms for all samples calcined at 200ºC are shown in Figure 4. The shapes of the isotherms are composite type I and type II isotherms (Kooli *et al.*, 1997; Sychev *et al.*, 2000). The Ti-PILCs isotherms correspond to low relative pressure values (below 0.03), to type I according to the Brunauer, Deming, Derning and Teller (BDDT) classification (Sing *et al.*, 1985) . This isotherm type is characteristic of a microporous system. Nevertheless, isotherms correspond to the type II class for higher P/P_o values, which is characteristic of systems with a large pore-size range (Kostoglod *et al.*, 1998). On the other hand, the isotherm of the original clay corresponds to type IV and is characteristic of materials having relatively large pores or non-porous materials. The isotherm plateau allows us to deduce the internal surface area by considering a monolayer adsorption of N_2 molecules. The presence of a hysteresis loop in all of the isotherm measurements indicates some degree of mesoporosity in these materials. According to Hutson (1999), the mesoporosity arises from stacking defects inherent in the clay itself, as evidenced by the hysteresis loop seen in the adsorption isotherm of the unpillared clay. These stacking defects are the result of the attraction between negatively charged basal surfaces and positively charged crystal edges to form an internal "house of cards" structure (Van Olphen, 1963). The

https://doi.org/10.1346/CCMN.2003.510105 Published online by Cambridge University Press

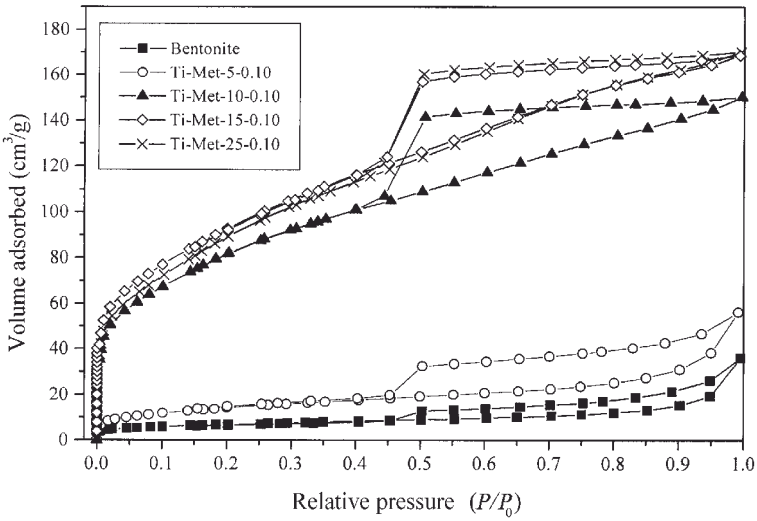

Figure 4. N_2 adsorption-desorption isotherms of the samples prepared using 5, 10, 15 and 25 mmoles Ti/g clay.

hysteresis loop corresponds to type H3 in the International Union of Pure and Applied Chemistry (IUPAC) classification, characteristic of materials whose pores are in the form of cracks. This finding is consistent with the structure expected for materials prepared by expanding a laminar structure (Monkaya and Jones, 1995). Figure 4 shows that the Ti-PILC prepared with 5 mmoles Ti/g clay is hardly pillared and shows an isotherm very similar to that of the original clay.

As far as thermal behavior is concerned, the sample Ti-Met-15-0.10 was selected in order to establish a comparison with the thermal properties of the original clay (see Figure 5). The results are quite similar for all the Ti-PILCs obtained. It can be seen that the original clay undergoes an acute weight loss at temperatures between 600 and 700ºC, due to the dehydroxylation of the structure. In the Ti-PILCs, however, this marked weight loss is not observed and the change is gradual as the temperature increases. The TGA plot of the original clay shows a loss of 9 wt.% below 150ºC and this is due to dehydration (loss of physically adsorbed water). Between 150 and 500ºC a very small (0.96 wt.%) weight loss is observed and this is attributed to the removal of interlayer water and the onset of dehydroxylation (Kloprogge *et al.*, 1994). The dehydroxylation process caused a maximum weight loss of 6 wt.% between 500 and 875ºC. Pillared clays lost approximately the same weight below 150ºC (9 wt.%) as did the original clay (this is not a representative value since it depends on the sample conditions before the analysis). Nevertheless, within the range 150–500ºC the weight loss was greater (5 wt.%) than for the original clay, a fact attributed to the removal of excess water absorbed within the pillared interlayer region and dehydroxylation of the pillars (Occelli and Tindwa, 1983). Dehydroxylation continues between 500 and 875ºC with the the weight loss being

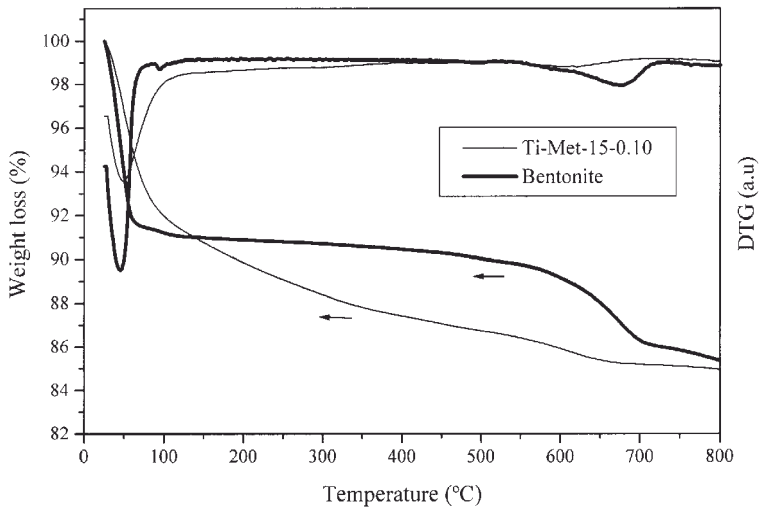

Figure 5. TG and DTG curves of original clay and Ti-Met-15-0.10.

https://doi.org/10.1346/CCMN.2003.510105 Published online by Cambridge University Press

smaller than that seen in the original clay (2.5 wt.%). As a result, only a small step is observed up to ~600ºC. The stability of the pillars is related to their dehydroxylation and as this becomes more marked so the basal spacing values decrease. This process can be seen in Figure 2b, where the d_{001} peak disappears at 600ºC as a result of the collapse of the structure.

According to the results above, samples obtained using 15 mmoles Ti/g clay that showed the best properties, were used as a reference in the next section.

Effect of the suspension clay concentration

Figure 1c shows the XRD traces corresponding to the materials prepared using clay suspensions of different concentrations (0.10, 0.13 and 0.20 wt.%), together with the pattern of the original clay for comparison (all samples were calcined at 500ºC). The d_{001} peaks of the resulting materials were found to shift towards the lower 2θ region, a clear indication of an increase in the basal spacing of the clay. A wider peak can also be observed at 7º2θ but this is less intense than the first peak. The broader peak corresponds to an interlayer spacing ranging from 3 to 4 Å. The basal spacing values are very similar in the three prepared solids and this is not unexpected given that the pillaring species in all three cases should be similar. It can also be observed that the basal spacing is not significantly affected by the calcination temperature (Table 2). This fact suggests that the Ti species are deposited principally between the silicate layers (Yamanaka *et al.*, 1987) but it is quite conceivable that some of the Ti polymers remain at the morphological surface of the clay crystallites.

A significant increase in the BET surface area is seen in the pillared samples and this confirms that the pillaring process has occurred (Table 3). The values obtained in the three samples are quite similar, although slightly higher in the sample prepared using a clay suspension of 0.13 wt.%. The micropore area of all the samples constitutes ~90% of the total surface area. The total acidity of the samples can be explained on the basis of the micropore surface area and the Ti content. The decrease in both the Ti content and the micropore area is responsible for the small total acidity value. This situation explains the fact that sample Ti-Met-15-0.13, which showed a favorable combination of these two effects, has the largest acidity value (Table 3).

In order to analyze the microporosity of the pillared clays, the N_2 adsorption properties over a range of pressure needed to be studied (Gil and Montes, 1997). The Horvath–Kawazoe (H-K) equation for slit-pore geometry was used to determine the micropore distribution. The micropore size-distribution for sample Ti-Met-15-0.13 is represented in Figure 6a. The Ti-PILC studied, and in general the rest of Ti-PILCs, contained a bimodal pore-size distribution that is in good agreement with the Dubinin-Radushkevich (D-R) plot results (not shown). This plot shows two deviations from linearity, suggesting the presence of two types of micropore. This bimodal size distribution for Ti-PILCs is consistent with previously reported distributions for similar clays (Hutson, 1999; Gil *et al.*, 1994; Hutson *et al.*, 1998). The micropore size-distribution is centered around two peaks: 5.2 and 9 Å. The interlayer spacing for these pillared clays was ~15–16 Å. Given that the micropores have a distribution centered around 5 and 9 Å, it is clear that the micropore size is limited by the interpillar distance rather than by the interlayer distance. The accuracy of the calculation of the micropore size-distribution by the Horvath–Kawazoe equation is very dependent on the accuracy of the calculation of the H-K interaction parameters and on the actual accessibility of the microporous pillared clays. However, the results showing a bimodal pore-size distribution and the corresponding micropore volumes are consistent with the results of the evaluation using the D-R equation.

The mesoporosity of sample Ti-Met-15-0.13 was characterized using the Barrett-Joyner-Halenda (BJH) method (Figure 6b). The mesopore size-distribution of this sample, and in general the rest of the prepared Ti-PILCs, showed a unimodal and narrow peak centered at 40 Å. The mesoporosity is from stacking defects inherent to the clay itself (as evidenced by the hysteresis loop of the adsorption isotherm from the unpillared clay). These stacking defects are the result of the attraction of negatively charged basal surfaces and positively charged crystal edges to form an internal "house of cards" structure (Hutson *et al.*, 1998). The mesopore structure of the Ti-pillared clays is not

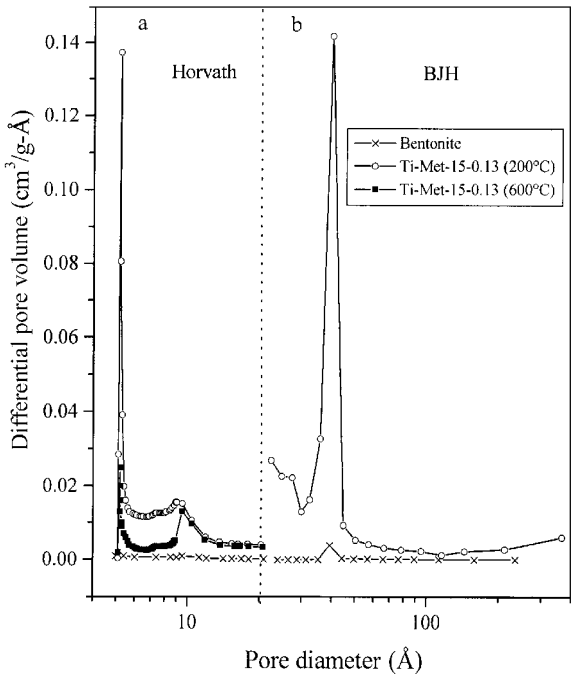

Figure 6. Micropore and mesopore size-distribution for Ti-Met-15-0.13.

https://doi.org/10.1346/CCMN.2003.510105 Published online by Cambridge University Press

significantly affected by the synthesis conditions employed during the pillaring process since this mesoporosity is present in the original clay.

In relation to the effect of calcination temperature, it can be observed in Figure 6a that the micropore distribution for Ti-PILCs calcined at 600ºC tends to have much less intense and flatter distributions than those for clays calcined at 200ºC. This is due to the collapse of pillars which reduces the interlayer distance and sintering of the pillars and decreases the micropore volume at higher temperature (Hutson, 1999).

The TPR profiles of the original clay and the Ti-PILC used as a reference (Ti-Met-15-0.13), both calcined at 200 and 500ºC, are given in Figure 7. The TPR profile of an Al-pillared clay is also shown for comparison. The peaks that appear at temperatures >600ºC cannot be stated with confidence to have originated from the reduction of some metallic species. They are probably caused by thermal decomposition of the material; indeed the structure collapses at 600–700ºC, as mentioned above (Figure 2b). In the original clay, a small shoulder appears at temperatures of ~520ºC and this was assigned to the reduction of Fe species present in the clay. This shoulder becomes more prominent in the pillared sample and is shifted to lower temperatures. At first we thought that the change in intensity produced in this peak was a result of the pillaring process, but it could also be caused by the reduction of Ti^{4+} to Ti^{3+}, which has a reduction potential that is sufficiently low to be feasible at this temperature. In order to verify this possibility, a pillared clay without Ti (Al-PILC) was analyzed by TPR. In this case, the existence of the shoulder was also observed and so the idea that it originated through reduction of Ti species could be discounted. The fact that this peak appears at lower temperatures in the pillared samples could be related to the internal diffusion-controlled phenomena since for pillared samples an enlargement of the basal spacing has taken place and, as a consequence the H_2 diffusion is faster, a situation that would help to close the gap between true and detected reduction temperatures. Finally, significant changes in the reduction peaks are not observed on comparing samples calcined at 200 and 500ºC. This fact seems to be related to the similar basal spacing obtained at both temperatures, a structural characteristic that allows H_2 molecules to diffuse in a very similar way in both cases.

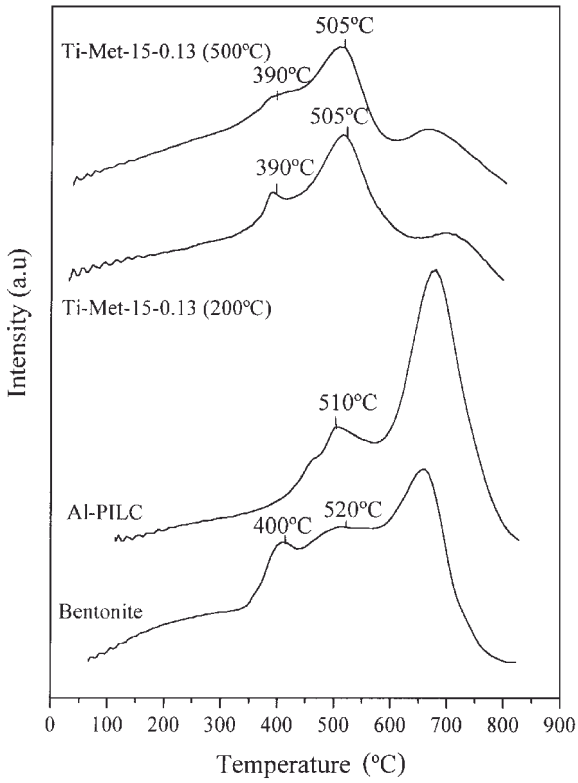

Figure 7. TPR profile for Ti-Met-15-0.10.

CONCLUSIONS

The results presented allow a series of experimental conditions, such as Ti alkoxide, Ti content and suspension clay concentration, to be tailored to prepare Ti-pillared clays that are stable at high temperatures. The synthesis conditions are extremely critical in that the morphology and texture of the final product may be dramatically modified on changing the conditions. The use of Ti methoxide allows the synthesis of Ti-pillared clays that have a large basal spacing, a notable degree of thermal stability and significant acidity in comparison to materials derived from other Ti alkoxides. The total acidity of pillared samples increased as both the Ti content and the micropore area increased. The surface area, the pore and micropore volume, the acidity and the d_{001} peak intensity increased upon increasing the amount of Ti added in the preparation (up to about 15 mmoles of Ti/g clay). It was possible to increase the clay concentration of the suspension to 0.13 wt.% of clay. Finally, the Ti-PILCs described here showed excellent thermal stability. At temperatures >500ºC the microporosity was affected and the interlayer spacing was reduced owing to collapse of the Ti oxide pillars.

ACKNOWLEDGMENTS

Financial support from the European Commission (Contract ERK5-CT-1999-00001) is gratefully acknowledged.

REFERENCES

Baes, C.F. and Mesmer, R.E. (1976) *The Hydrolysis of Cations*. Wiley, New York.

Bagshaw, S.A. and Cooney, R.P. (1993) FTIR surface site analysis of pillared clays using pyridine probe species. *Chemistry of Materials*, **5**, 1101–1109.

Bahranowski, K. and Serwicka, E.M. (1993) ESR study of vanadium-doped alumina and pillared montmorillonites. *Colloids and Surfaces A*, **72**, 153–160.

https://doi.org/10.1346/CCMN.2003.510105 Published online by Cambridge University Press

Barrer, R.M., Joyner, L.G. and Halenda, P.P. (1951) The determination of pore volume and area distribution in porous substances. *Journal of the American Chemical Society*, **73**, 373–380.

Bernier, A., Admaiai, L.F. and Grange, P. (1991) Synthesis and characterization of titanium pillared clays. Influence of the temperature of preparation. *Applied Catalysis*, **77**, 269–281.

Bovey, J., Kooli, F. and Jones, W. (1996) Preparation and characterization of Ti-Pillared acid-activated clay catalysts. *Clay Minerals*, **31**, 501–506.

Burch, R. (1988) Introduction. *Catalysis Today*, **2**, 185–186.

Cañizares, P., Valverde, J.L., Molina, C.B., Rodriguez, L. and Sánchez, P. (1999) Synthesis and characterization of PILCs with single and mixed oxide pillars prepared from two different bentonites. A comparative study. *Microporous and Mesoporous Materials*, **29**, 267–281.

Chevalier, S., Franck, R., Suquet, H., Lambert, J.F. and Barthomeuf, D. (1994) Al-pillared saponites. *Journal of the Chemical Society*, **90**, 667–674.

Clearfield, A. (1994) Pillaring studies on the some layered oxides with Ruddlesden-copper related structures. *Journal of Solid State Chemistry*, **112**, 288–294.

Del Castillo, H.L. (1993) Preparation and catalytic activity of titanium pillared montmorillonite. *Applied Catalysis A: General*, **103**, 23–34.

Del Castillo, H.L., Gil, A. and Grange, P. (1996) Selective catalytic reduction of NO by NH_3 on titanium pillared montmorillonite. *Catalysis Letters*, **36**, 237–239.

Del Castillo, H.L., Gil, A. and Grange, P. (1997) Influence of the nature of titanium alkoxide and of the acid of hydrolysis in the preparation of titanium pillared montmorillonites. *Journal of Physics and Chemistry of Solids*, **58**, 1053–1062.

Einaga, H. (1979) Hydrolysis of titanium(IV) in aqueous (Na,H)Cl solution. *Journal of the Chemical Society, Dalton Transactions*, 1917–1919.

Gil, A. and Montes, M. (1997) Metathesis of propene on molybdenum-alumina-pillared montmorillonite. *Industrial & Engineering Chemistry Research*, **36**, 1431–1443.

Gil, A., Diaz, A., Montes, M. and Acosta, D.R. (1994) Characterization of the microporosity of pillared clays by nitrogen adsorption. Application of the Horvath–Kawazoe approach. *Journal of Materials Science*, **29**, 4927–4932.

Horvath, R. and Kawazoe, K.J. (1983) Method for the calculation of effective pore size distribution in molecular sieve carbon. *Chemistry Engineering Japan*, **16**, 470–475.

Hutson, N.D. (1999) Control of microporosity of Al_2O_3-pillared clays: effect of pH, calcination temperature and clay cation exchange capacity. *Microporous and Mesoporous Materials*, **28**, 447–459.

Hutson, N.D., Gualdoni, D.J. and Yang, R.T. (1998) Synthesis and characterization of the microporosity of ion-exchanged Al_2O_3 pillared clays. *Chemistry of Materials*, **10**, 3707–3715.

Kloprogge, J.T. (1998) Synthesis of smectites and porous pillared clay catalysts: A review. *Journal of Porous Materials*, **5**, 5–41.

Kloprogge, J.T., Booy, E., Jansen, J.B.H. and Geus, J.W. (1994) The effect of thermal treatment on the properties of hydroxy-Al and hydroxy-Ga pillared montmorillonite and beidellite. *Clay Minerals*, **29**, 153–167.

Kooli, F., Bovey, J. and Jones, W. (1997) Dependence of the properties of titanium-pillared clays on the host matrix: a comparison of montmorillonite, saponite and rectorite pillared materials. *Journal of Materials Chemistry*, **7**, 153–158.

Kostoglod, N.Y., Sychev, M.V., Prikhod'ko, R.V., Astrelin, I.M., Stepanenko, A.V. and Rozwadowski, M. (1998) Porous structure of pillared clays II. Montmorillonte pillared with titanium dioxide. *Kinetics and Catalysis*, **39**, 547–553.

Lahav, N., Shani, U. and Shabtai, J. (1978) Cross-linked smectites. I: Preparation and properties of some hydroxy-aluminum montmorillonite. *Clays and Clay Minerals*, **26**, 107–115.

Li, W., Sirilumpen, M. and Yang, R.T. (1997) Selective catalytic reduction of nitric oxide by ethylene in the presence of oxygen over Cu^{2+} ion-exchanged pillared clays. *Applied Catalysis B: Environmental*, **11**, 347–363.

Long, R.Q. and Yang, R.T. (2000) Catalytic performance and characterization of VO^{2+}-exchanged titania pillared clays for selective catalytic reduction of nitric oxide with ammonia. *Journal of Catalysis*, **196**, 73–85.

Malla, P., Yamanaka, S. and Komarneni, S. (1989) Unusual water vapor adsorption behaviour of montmorillonite pillared with ceramic oxides. *Solid State Ionics*, **32/33**, 354–362.

Monkaya, R. and Jones, W. (1995) Pillared clays and pillared acid-activated clays: A comparative study of physical, acidic and catalytic properties. *Journal of Catalysis*, **153**, 76–85.

Nabivanets, B.I. and Kudritskaya, L.N. (1967) A study on the polymerization of titanium (IV) in hydrochloric acid solutions. *Russian Journal of Inorganic Chemistry*, **12**, 616–620.

Occelli, M.L. and Tindwa, R.L. (1983) Physicochemical properties of montmorillonite interlayered with cationic oxyaluminum pillars. *Clays and Clay Minerals*, **31**, 22–28.

Pesquera, C., González, F., Benito, I., Mendioroz, S. and Pajares, J.A. (1991) Synthesis and characterization of pillared montmorillonite catalysts. *Applied Catalysis*, **69**, 97–104.

Purnell, J.H. (1990) Current trends and applications. Pp. 107–112 in: *Pillared Layered Structures* (I.V. Michell, editor). Elsevier Applied Science, London & New York.

Shabtai, J., Rosell, M. and Tokarz, M. (1984) Cross-linked smectites III. Synthesis and properties of hydroxy-aluminum hectorites and fluorhectorites. *Clays and Clay Minerals*, **35**, 99–107.

Sing, K.S.W., Everett, D.H., Haul, R.A.W., Moscou, L., Pierotti, R.A., Rouguerol, J. and Siernieniewska, T. (1985) Reporting physisorption data for gas/solids systems with special reference to the determination of surface area and porosity. *Pure and Applied Chemistry*, **57**, 603–619.

Sprung, R., Davies, M.E., Kauffman, J.S. and Dybowsky, C. (1990) Pillared magadiite with silicate species. *Industrial Engineering Chemistry Resource*, **29**, 213–220.

Sterte, J. (1986) Synthesis and properties of titanium oxide cross-linked montmorillonite. *Clays and Clay Minerals*, **34**, 658–664.

Sun Kou, M.R., Mendioroz, S. and Muñoz, V. (2000) Evaluation of the acidity of pillared montmorillonites by pyridine adsorption. *Clay and Clay Minerals*, **48**, 528–536.

Sychev, M. (1992) Titania pillared montmorillonite (TiPILM): sorption and spectroscopic characterization. Pp. 63–65 in: Proceedings of the Symposium *"Characterization and properties of zeolitic materials"* of the Polish-German Zeolite Colloquium (M. Rozwadowski, editor). Torun, Poland.

Sychev, M., Shubinaa, T., Rozwadowskib, A.P.B., Sommene, V., De Beerc, H.J. and Van Santenc, R.A. (2000) Characterization of the microporosity of chromia and titania-pillared montmorillonites differing in pillar density. *Microporous and Mesoporous Materials*, **37**, 187–200.

Van Olphen, H. (1963) *An Introduction to Clay Colloid Chemistry*, 2nd edition. Wiley, New York.

Vicente, M.A., Bañares-Muñoz, M.A., Toranzo, R., Gandía, L.M. and Gil, A. (2001) Influence of the Ti precursor on the properties of Ti-pillared smectites. *Clay Minerals*, **36**, 125–138.

Yamanaka, S. and Brindley, G.W. (1979) High surface area

solids obtained by reaction of montmorillonite with zirconyl chloride. *Clays and Clay Minerals*, **27**, 119–124.

Yamanaka, S., Nishihara, T., Hattori, M. and Suzuki, Y. (1987) Preparation and properties of titania pillared clay. *Mathematics, Chemistry and Physics*, **17**, 87–101.

Yang, R.T., Chen, J.P., Kikkinides, E.S., Cheng, L.S. and Cichanowicz, J.E. (1992) Pillared clays as superior catalysts for selective catalytic reduction of nitric oxide with ammonia. *Industrial Engineering Chemistry Resource*, **31**, 1440–1445.

Zhu, H.Y., Gao, W.H. and Vansant, E.F. (1995) The porosity and water adsorption of alumina-pillared montmorillonite. *Journal of Colloids and Interface Science*, **171**, 377–385.

(*Received 11 January 2002; revised 1 August 2002; Ms. 634; A.E. James E. Amonette*)